RSC Advances

REVIEW

View Article Online
View Journal | View Issue

Cite this: *RSC Adv.*, 2024, **14**, 30618

Unveiling the potential of emergent nanoscale composite polymer electrolytes for safe and efficient all solid-state lithium-ion batteries

Adhigan Murali, [ad] R. Ramesh,*[b] Mohan Sakar, [c] SeonJoo Park*[a] and Sung Soo Han*[d]

Received 16th July 2024
Accepted 12th September 2024

DOI: 10.1039/d4ra05134c

rsc.li/rsc-advances

Solid-state polymer electrolytes (SSPEs) are promising materials for Li-ion batteries due to their enhanced safety features, which are crucial for preventing short circuits and explosions, replacing traditional liquid electrolytes with solid electrolytes are increasingly important to improve battery reliability and lifespan. There are essentially three-types of solid-state electrolytes such as solid polymer electrolyte, composite based polymer electrolyte and gel-based polymer electrolyte are largely used in battery applications. Additionally, battery separators must have high ionic conductivity and porosity to boost safety and performance. Durable solid composites electrolytes with excellent thermal and mechanical properties are key to reducing the risk of lithium dendrite growth, thereby improving overall battery efficiency. Despite their potential, challenges like scalability, cost and real-world performance optimizations still need to be addressed.

1. Introduction

Lithium-ion (Li-ion) based batteries are considered among the most prominent high-performance energy devices. In 1990, Sony commercialized their first ever Li-ion batteries in the world. These lithium-ion batteries have wide applications over the heavy electrical vehicles (EV), electronic portable based mini gadgets and energy storages, where they have also been undergone various progressions over the years.[1] In this direction, it is realized that the SPEs can considerably reduce the cost of Li-ion batteries *via* substituting the predictable liquid electrolytes.[2] The use of polymer solid packages with good tensile strength and resistors with positive temperature coefficient is not important for Li-ion batteries. The fabrication cost of SPEs is considerably lower than that of liquid electrolytes. Polymer based electrolytes such as polyethylene oxide (PEO), poly(ether ether ketone), polyvinylidene fluoride (PVDF), polycarbonates (PC), polymethyl methacrylate (PMMA), poly acrylonitrile (PAN), where they essentially used as polymer matrix in the lithium ion batteries.[3] Amongst, the PEO is a common polymer matrix in Li-ion batteries (LIBs). PEO has improved chain flexibility, superior electrochemical stability, possesses good solubility in conductive lithium salts along with low glass transition temperature (T_g) and therefore, it is considered as a potential and good polymer host for LIBs. Though, the poor electrolyte interfaces and low crystalline nature at low temperature hinder the ionic conductivity of PEO (10^{-8} to 10^{-6} S cm^{-1}) to be conveniently used in LIBs.[4,5] To overcome this, PEOs is frequently blended with another polymers, or included with some fillers-nano based/plasticizers in order to improve its ionic conductivity. Furthermore, dioctyl phthalate, dibutyl phthalate and dimethyl phthalates are commonly used as a plasticizer with PEO–$LiClO_4$ host matrix to improve the ionic conductivity (10^{-5} S cm^{-1}).[6] Chakrabarti *et al.*, incorporated a borate ester (star-configure) into a PEO matrix, which achieved an ionic transport of 9.1×10^{-5} S cm^{-1} at 30 °C.[7] Yongku *et al.*, improved conductivity in a photocured PEO electrolyte by incorporating poly(ethylene glycol)dimethyl ether and achieved their ionic conductivity up to 5.1×10^{-4} S cm^{-1} at 30 °C, where it was realized that it can be operated at ambient temperature.[8] Similarly, an inorganic ceramic-based electrolyte composed of garnet type $Li_7La_3Zr_2O_{12}$ (LLZO) and $Li_{6.4}La_3Zr_{1.4}Ta_{0.6}O_{12}$ (LLZTO) showed excellent ionic conductivity above 10^{-4} S cm^{-1}. These inorganic ceramics also showed good thermal and electro-chemical durability. Because of their brittle and rigidity, it showed poor contact with electrodes and hence, a highest interfacial resistance between electrodes and electrolyte was created.[9,10] Cha *et al.*, established a composite based polymer electrolyte for LIBs. This electrolyte involves of PEO matrix, $Li_7La_3Zr_2O_{12}$ nanofiller, and PEGDME based plasticizer was used. The 10 wt% of PEGDME with this composite exhibited the

[a]*Department of Life Sciences, Yeungnam University, 280 Daehak-Ro, Gyeongsan, 38541, Republic of Korea. E-mail: sjpark01@ynu.ac.kr*

[b]*Department of Chemical Engineering, School of Mechanical, Chemical and Material Engineering, Adama Science and Technology University, Adama, P.O. Box-1888, Adama, Ethiopia. E-mail: ramesh.redrouthu@astu.edu.et*

[c]*Centre for Nano and Material Sciences, Jain University, Bangalore 562112, Karnataka, India*

[d]*School of Chemical Engineering, Yeungnam University, 280 Daehak-Ro, Gyeongsan, 38541, Republic of Korea. E-mail: sshan@yu.ac.kr*

ionic transport of 4.7×10^{-4} S cm^{-1}.[11] On the other hand, it is found that the sulfide-based polymer electrolytes have high ionic transport compared that of the oxide, nitride and phosphide-based solid electrolytes. It is detected that the ionic mobility of the sulfide/PEO and sulfide/PVDF was 4×10^{-4} S cm^{-1} without lithium salt added, where it was further increased up to 7×10^{-4} S cm^{-1} with the accumulation of lithium.[12,13] Similarly, the glass ceramic glass-ceramic $78Li_2S$–$22P_2S_5$ (7822gc)-based composite solid polymer membrane reinforced matrix with 120 μm thickness was synthesized by Zhang, where the good ionic conductivities were estimated up to 2–4 x 10^{-4} S cm^{-1} for the synthesized various composite electrolyte membranes with different polymers and solvents. Among the materials, the $78Li_2S$–$22P_2S_5$ (7822) PVDF-LiTFSI-9703-EAC nanomembranes was noticed to have the highest ionic mobility of 7.07×10^{-4} S cm^{-1}.[12] Further, it is found that the PVDF could also be suitable polymer in developing the lithium ion batteries. Both the crystalline/amorphous natures of the PVDF have the benefited over the thermal stability and flexibility properties, which can be suitable to develop the solid electrolytes. Accordingly, the composite polymer electrolytes based on PVDF with various types of nanofillers PEG(PVP)–PVDF–X (X = LiF, Li_2So_4, LiCl, NaCl) have been prepared at room temperature. In this, the PVDF + NMP + LiCl compositions showed the highest ionic conductivity.[13] Thanks to the excellent electro-chemical stability and affinity of the electrolytes, the fluoro polymers have also been gained more attention on the Li-ion batteries. PVDF based nanofibrous polymer electrolytes containing the 1 mole of $LiPF_6$–ethylene carbonate/diethyl carbonate/dimethyl carbonate was synthesized, where the electrochemical-stability was found to be above 5.0 V and showed excellent cycle performances at C/2-rate at 60 °C.[14] However, the crystalline part of the polyvinylidene fluoride somehow hinders the ionic transport of the electrolytes. Some of the research works were demonstrated on the coating of inorganic particles on the surface of polyolefins to enhance the thermal stability and wettability. But the major drawback of the inorganic particles is that they would fall off easily.[15,16] For instance, the ZrO_2–40% PVDF membrane observed a higher discharge behavior of around 120 mA h g^{-1} and the ionic conductivity of 0.96 mS cm^{-1}. In this study, among the different wt% of PVDF–ZrO_2 fiber membranes, the 40% PVDF with zirconia fiber displayed the high porosity in the matrix.[17] Furthermore, the nanoparticle coated polyvinylidene fluoride membranes were found to be one of the most efficient separators, where they were used for high power Li-ion batteries with improved safety. In this direction, the inorganic materials such as TiO_2, SiO_2, Al_2O_3 and ZrO_2 based ceramic nanofillers were utilized to enhance the wettability and to rise the thermal properties of the solid electrolytes. The Al_2O_3/PVDF and PVDF/SiO_2 and PVDF/Al_2O_3/SiO_2 were synthesized by magnetron deposition and melt electrospinning techniques, where their ionic conductivities were estimated to be 1.309, 0.946, 2.055 mS cm^{-1} at 25 °C respectively.[18] The polyimide (PI) and polyacrylonitrile (PAN) are one of the efficient polymer matrixes, which possess great wettability and have good thermal stability. Polyimide is indeed recognized as a super-engineering plastic because of its exceptional thermal stability and strong mechanical properties. Accordingly, the P84 polyimide powder (50) + ethylene carbonate (50) and EC (50) + P84 (50) + $LiCF_3SO_3$ (lithium trifluoro methane sulfonate) electrolytes were synthesized with 2 and 4 wt% of $LiCF_3SO_3$. The electrolyte with 4% of lithium salt showed enhanced the conductivity by the order of two magnitudes as compared to the electrolyte that did not contain Li salt.[19] Polyimides have been used in many advanced technologies due to their outstanding thermo-oxidative and mechanical properties, where they also have good affinity with the organic solvents such as carbonates. Moreover, the PEO and polyimide-based polymer matrixes could be easily dissolved in various alkali metals, lithium trifluoro methane sulphonate ($LiCF_3SO_3$), lithium perchlorate ($LiClO_4$) and lithium tetrafluoroborate ($LiBF_4$), which have typically been used as lithium salts. Emre *et al.*,[20] fabricated the polyimide nanomembrane based high performance material reinforced photocured hybrid electrolytes. Benzophenone tetracarboxylic di-anhydride (BTDA) and 4,4′-oxydianiline (ODA), are combined together and followed by electrospinning and imidization method. Hybrid resin, comprising bisphenol A ethoxylate dimethacrylate (BEMA), PEGMA and 3-(methacryloyloxy)propyl trimethoxy silane (MAPMS), was used to dip the polyimide nanofibers, which were then photocured to prepare the polymeric membrane for the battery studies. The ionic conductivity was achieved up to 7.2×10^{-3} S cm^{-1} at atmospheric temperature and also showed better electrolyte uptake.[20] The light-weight and thin solid electrolytes are capable of achieving the energy density that comparable to the liquid electrolytes-based Li-ion batteries. Solid electrolytes with comparable thickness of 10 μm are being used in the commercial polymer electrolyte separators. Jiayu *et al.*, successfully fabricated 8.6 μm thick nano-porous polyimide loaded with PEO and LiTFSI salt, which was found to be suitable solid polymer composite based electrolyte for the Li-ion battery. The PI electrolyte film is fire-resistant and strong, helping to prevent batteries from short-circuiting even after cycling for more than 1000 h. Also, the developed PI/PEO/LiTFSI solid composite polymer electrolyte improved the ionic transport of 2.3×10^{-4} S cm^{-1}.[21] It is known that the separators should provide the channel for the ions to reciprocate between the cathode and anode electrodes to improve the ionic mobility, where the total quality of the battery is determined by the performance of the separator. The high-heat resistant polymers such as polyimide (PI), polyether ether ketone (PEEK), and polyacrylonitrile (PAN) can be used to replace the low melting point materials such as polyolefin. Owing to their good thermal resistance, these polymer-based separators could increase the dimensional stability and prevent the short circuiting and thermal runaway at higher temperatures.[22,23] In addition, they also have good compatibility and hydrophilicity, hence, it can be efficiently utilized as reinforcing materials in order to expand and enhanced their quality of the separators. Fig. 1 shows the various functional and chemical structures of the significant rich ether-oxygen, fluoro and carbonate-based polymers, which are potentially utilized as polymer host in polymer electrolytes for solid-state Li-ion batteries (SSLIBs).

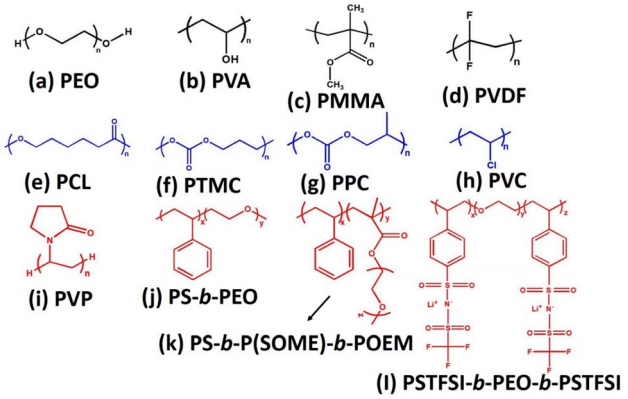

Fig. 1 Various polar polymers used as polymer electrolytes for SSLIBs, (a) PEO, (b) PVA, (c) PMMA, (d)PVDF, (e) PCL, (f) poly(trimethylene carbonate) (PTMC), (g) poly(propylene carbonate) (PPC), (h) poly(vinyl chloride), (i) poly(vinylpyrrolidone) (PVP), (j) polystyrene-*b*-poly-ethylene oxide (PS-*b*-PEO), (k) polystyrene-*b*-polystyrene-*grad*-poly(oligo-oxyethylenemethacrylate)-*b*-poly(oligo-oxy-ethylenemethacryalte) (PS-*b*-P(SOEM)-*b*-POEM), (l) poly(4-styrenesulfonyl)(trifluromethanesulfonyl imide)-*b*-polyethylene oxide-*b*-poly(4-styrenesulfonyl)(trifluoromethanesulfonyl imide) (PSTFSI-*b*-PEO-*b*-PSTFSI).

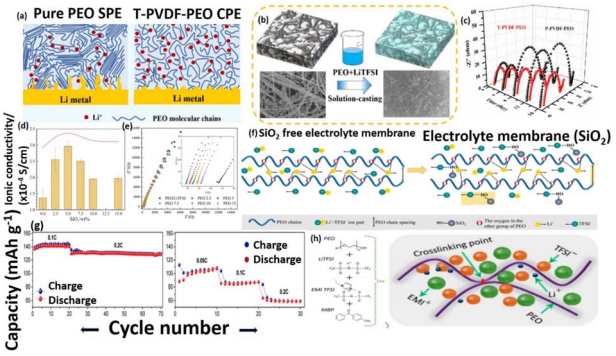

Fig. 2 (a) Schematic images of Li-ion conducting path using PEO with T-PVDF-PEO electrolyte in the all-solid-state batteries, (b) assembly of the root-soil-based all-solid composite electrolytes by casting method of PEO-LITFSI liquid converted into the T-PVDF nanofibers, (c) impedance spectroscopy of Li/T-PVDF-PEO/Li and Li/P-PVDF-PEO/Li in symmetric cell at 70 °C.[26] Reproduced ref. 26 with permission from Elsevier, Copyright 2020, (d) ionic conductivity, (e) impedance resistance of SS/SPE/SS at ambient temperature, (f) the mechanism of Li-ion mobility of polymer electrolytes.[27] Reproduced ref. 27 with permission from American Chemical Society, Copyright 2022, (g) Specific capacity *vs.* cycle number plot at different C rate at 55 °C, and 20 °C, (h) polymer electrolyte formed through interlinking polymer chain after UV exposure (imidazolium based RTIL).[28] Reproduced ref. 28 with permission from American Chemical Society, Copyright 2015.

2. Solid polymer electrolytes (SPEs)

The SPEs are mostly contain of even mixtures of solid polymer and salt of Li. SPEs consist of a host polymer network and salt of Li as solute without any accumulation of solvents as plasticizer. The polymer host matrix should fulfill some of the significant necessities for its usages as SPEs. SPEs must meet critical requirement, including promoting salt dissociation through cation solvation and having a high dielectric constant to facilitate efficient charge separation of salt. To facilitate the atomic motion of the polymer network, the high backbone flexibility is required. High molecular weight polymer matrix generally improves the mechanical strength significantly. Since last four decades, different polymer electrolytes were used for Li-ion batteries owing to their good mechanical and thermal behavior. Moreover, such kinds of polymers have better interfacial contact between the electrode/electrolytes as illustrated in Fig. 1. Dry solid polymer electrolytes, composed solely of the host matrix and Li salts, are readily available in the market at an affordable price. Most promising polymer matrix is PEO because of its elastic based ethylene oxide segmental points and rich ether oxygen. Most commonly used Li salts include $LiClO_4$, $LiAsF_6$, $LiPF_6$, $LiCF_3SO_3$, $LiBF_4$, and $LiN(CF_3SO_2)_2$. The mobility ions in these systems will be in the order of $LiBF_4 > LiClO_4 > LiPF_6 > LiAsF_6 > LiCF_3SO_3 > LiN(CF_3SO_2)_2$. Similarly, the dissociation constants will be in the order of $LiN(CF_3SO_2)_2 > LiAsF_6 > LiPF_6 > LiClO_4 > LiBF_4 > LiCF_3SO_3$. As it is known that the PEO is excellent conducting electrolyte, which can effectively be used for Li-ion batteries.[24,25] In that direction, Lu *et al.*, developed the root-soil-like PEO based composites for long-cycle capability and free-dendrite of solid Li-metal battery.[26] PVDF based nanofiber with multi structure has been incorporated onto the PEO network in order to developed the solid-state based root-soil based composites electrolyte. The possible Li conducting pathway, interaction between T-PVDF (tetrabutylammonium chloride in PVDF fiber) and root soil like composites preparation was clearly shown in Fig. 2a and b. The outcome of this work, the composite electrolyte shows excellent electrochemical behavior, the Li symmetric battery voltage remained stable at 70 mV for 1000 h below 0.3 mA cm^{-2}. Moreover, the interface impedance of Li/Li symmetric battery was increased their storage time and the interface resistance changes from 47.40 and 46.01 to 147.61 and 143.80 respectively, the composite has better interface compatibility between multi structure composites-based electrolytes and Li metal to better extent as illustrated in Fig. 2c. Similarly, Yang *et al.*, fabricated the solvent-free PEO/LiTFSI/SiO_2 composite based electrolytes with outstanding ionic conductivity for all-solid-state batteries.[27] They incorporated the silica and LiTFSI onto PEO matrix by an eccentric rotor mixer under flow elongational field. The outcome of this work, the prepared composite electrolytes exhibited high ionic mobility (10^{-4} S cm^{-1}) due to the presence of Li salt and SiO_2 (uniform dispersion on the electrolytes) as shown in Fig. 2d and e. Also, the charge–discharge of the coulomb efficiency up to 100% even after 90 cycles, and moreover, discharge specific capacity feebly reduced, which denoted as good electrochemical performance. The presence of SiO_2 onto polymer matrix, how the silica behaves under elongational flow field and their detailed mechanism has been given in Fig. 2f.

Nair *et al.*, reported the rich ionic conductive, self-standing and tack-free ethylene oxide electrolyte containing room temperature ionic liquid (RTIL) with Li salt are successfully prepared under UV irradiation. The formed composite within

the membrane free radical can combine with another free radical from the same chain or a neighboring chain, which created a cross-linked network (see Fig. 2h).[28] The constant current charge/discharge was carried out at increasing cycles rates at mild temperature (20 °C and 55 °C) and it enhanced their cyclic stability, which related to the typical biphasic Li^+ extraction/insertion mechanism in chosen active materials as shown in Fig. 2g. One key factor affecting polymer–metal ion interaction is the functional group on the polymer matrix backbone, degree of branching, molecular weight and compositions. The plasticizers are used to decrease the crystallinity by making the PEO matrix amorphous nature at low temperature. The conductivity of the PEO polymer matrix could be increased significantly by incorporating the plasticizers namely succinonitrile, ethylene carbonate and propylene carbonate *etc.* In this context, the Li/SPE/$LiMn_2O_4$ and Li/SPE/$LiCoO_2$ cells were fabricated and those SPEs were consisted of PEO as the host matrix and the poly(ethylene glycol) dimethyl ether as a plasticizer to enhance the ionic transport.[8] Another way of improving the ionic transport of the host polymer matrices is to use the grafted polymers or block copolymers as a polymer matrix. Grafting of functional branches in the backbone of the main polymer chain is called grafting. Quichao *et al.*, reported the grafted copolymer-based electrolytes consisting of poly(oxyethylene)methacrylate-*g*-poly(dimethyl siloxane) doped with lithium triflate. This kind of grafted SPE[29–31] can be used in an extensive range of temperatures up to 120 °C and above.[32] Trapa *et al.*, fabricated an amphiphilic graft copolymer electrolyte with poly(oxyethylene) methacrylate block (hydrophilic) and a polydimethyl siloxane block (hydrophobic). This polymer was withstood up to 250–300 °C without decomposing.[33] The grafted polymer electrolytes are typically not flammable unlike gel polymer electrolytes and plasticized electrolytes. Hence, this grafted polymer electrolyte does not kick up fire hazards.

3. Composite polymer electrolytes (CPEs)

Generally, the inorganic nanofillers are supplementary to the solid polymer electrolytes to develop the composite based polymer electrolytes to progress the mechanical property and ionic transport. The type of fillers used to make composite polymer electrolytes are inorganic fillers, organic fillers, ceramic fillers and nano fillers. The costs of these fillers are low and these fillers are biodegradable. Organic fillers tend to enhance both the mechanical and thermal properties of composite polymer solid electrolytes, improving aspects such as dimensional stability, rigidity and toughness. Two types of nanofillers are utilized in CPEs. They are non-ionically conductive fillers (passive) and ionically conductive fillers (active).[34–37]

3.1. Non-ionically conductive filler based CPEs

Various studies have been done in incorporating the non-ionically conductive nanoparticles as fillers with the polymer electrolyte to enhanced the mechanical strength and to enhance the ionic mobility simultaneously. The reduction in the crystallinity enhances the ionic transport of a polymer matrix.[38] Al_2O_3 and SiO_2 are some of the examples for the non-ionically conductive nanoparticles that incorporated in the solid electrolytes to rise the ionic conductivity. In addition, some ferroelectric ceramic-based nanofillers namely, $PbTiO_3$, $BaTiO_3$, $LiNbO_3$, and $SrBi_4Ti_4O_{15}$ have also been used in the polymer based solid electrolyte to enhanced the ionic conductivity. The surface charge of the ferroelectric can generate the high number of amorphous phases. Hence, this will enhance the overall ionic conductivity of the system. For instance, the ferroelectric nano-$BaTiO_3$ was used as nanofiller in PVA_C/PVDF–HFP to develop the lithium ion batteries. Consequently, the ionic conductivity was significantly enhanced when 75 wt% of the $BaTiO_3$ nanofillers were used in CPEs. This $BaTiO_3$-based nanofiller displayed a very high electric constant, which effectively helped for the dissociation of Li salt to enhance the charge carrier concentrations in the polymer electrolyte matrix.[39] The ceramic fillers can be reduced the degree of polymer crystallinities and support the lithium ions for their fast transport. Another example is that the usage of porous polyphosphazene as nanotube fillers in PEO-based composites based solid polymer electrolytes. With an accumulation of PZS nanotubes, the Li-ion transport number, ionic conductivity, and electrochemical durability window were increased and the conductivity was also increased.[40] Also, Al_2O_3-based nanofillers have also been used in CPE based electrolytes in lithium ion batteries. An organic–inorganic composite polymer electrolyte (PEO–$LiClO_4$) was employed in Li-ion batteries. Such nanofillers utilized in Li-ion battery exposed that the nanofillers generally tend to enhanced the conductivity, ion migration towards anode and cathode and their direction in the Li-battery.[41] In this way, other work the utilization of organic based polymer nanofillers based amorphous PEO based electrolyte, found that the hydrolyzed polymaleic anhydride can greatly overwhelm the crystallinity of PEO. Accordingly, the ion mobility of PEO based on the polymer electrolytes was also increased to around 1.13×10^{-4} S cm^{-1} at 35 °C. Generally, the PEO solid electrolytes displayed poor ionic conductivity and high temperature-related limitation in solid-state batteries, the researcher employed hydrolyzed polymaleic anhydride (HPMA) in combination with an organic polymer filter. This approach reduced crystallinity and significantly improved the ionic transport of PEO-based composite polymer solid electrolyte.[42] Different polymer composite based separators, solvents, mechanical strength, ionic conductivities are clearly tabulated in Table 1.

3.2. Accelerating ion transport with CPEs

Fast-ionic conductors-based composites polymer electrolytes have emerged as a highly attractive solution in the advancement of LIBs. With their anti-flammable nature and remarkable ability to boost ionic transport reached 10^{-2} S cm^{-1}. Such electrolytes hold tremendous potential for revolutionizing battery technology.[64] The sulfides ($Li_{10}GeP_2S_{12}$), garnet type ($Li_7La_3Zr_2O_{12}$ (LLZO)), and NASICON ($Li_{1.5}Al_{0.5}Ge_{1.5}(PO_4)_3$) are rapid ionic conductors utilized in CPEs. Li *et al.*, reported

Table 1 Different composite separators for solid Li-ion batteries

Polymer matrix	Composite material	Solvents	Tensile strength	Ionic transport	Efficiency	Ref.
PI	SiO_2	$LiPF_6$–EC/DMC	4.7 MPa	2.27 mS cm^{-1}	Good electrolyte affinity, thermal properties	43
PI	Al_2O_3	$LiPF_6$–EC/DMC	38.6 MPa	—	Better mechanical strength and thermal stability	44
PI	—	1 mole $LiPF_6$–(EC + EMC + DMC)	4.17 MPa	2.0×10^{-3} S cm^{-1}	Good electrochemical stability up to 5.0 V	45
PAN	HFP–PVDF	$LiPF_6$–DEC/EC/EMC	18.9 MPa	1.74 mS cm^{-1}	Better electrolyte attraction, tensile strength, electrochemical stable battery efficiency	46
PAN	PUs	$LiPF_6$–DMC/EC/EMC	10.4 MPa	2.07 mS cm^{-1}	Better electrolyte attraction and tensile strength	47
PI	HFP–PVDF	DMC/$LiPF_6$–EC	53 MPa	1.68 mS cm^{-1}	Enhanced mechanical strength and thermal and cycling stability	48
PVDF	PI	$LiPF_6$–EC/DEC/PC/VC	—	1.3 mS cm^{-1}	Good cycling stability and thermal stability	49
PI	ZSM-5	—	—	1.04 mS cm^{-1}	Good thermal stability and improved electrochemical property	50
PMMA/PVDF–HFP	$MgAl_2O_4$J	EC/DEC–$LiPF_6$	—	1.40–2.60 mS cm^{-1}	Enhanced electrolyte affinity	51
PVDF/PMMA	SiO_2	—	32 MPa	4.0 mS cm^{-1}	Enhanced battery charge–discharge capacity and C-rate performance and good tensile strength and thermal stability	52
PAN	SiO_2	$LiPF_6$–EC/EMC	3.5–4.5 MPa	2.1–2.6 mS cm^{-1}	Better battery C-rate performances and thermal stabilities	53
PVDF	SiO_2	$LiPF_6$–EC/EMC	~13 MPa	2.1–2.6 mS cm^{-1}	Good battery C-rate performance and enhanced electrolyte affinity	54
PVDF	MMT	$LiPF_6$–EC/EMC/DMC	2.1–3.3 MPa	2.58–4.2 mS cm^{-1}	Good battery cycling stabilities and better electrolyte affinities	55
Nylon 6,6	SiO_2	$LiPF_6$–EC/EMC	22 MPa	3.1–3.8 mS cm^{-1}	Good battery cycling stability and electrolyte affinity and good tensile strength	56
Nylon 6,6	TiO_2	$LiPF_6$–EC/EMC	~22 MPa	3.3 mS cm^{-1}	Good battery cycling stability and electrolyte affinity And good mechanical strength	57
PVDF	ZSM-5	$LiPF_6$–EC/EMC/DMC	3.2 MPa	1.72 mS cm^{-1}	Good battery cycling stability and electrolyte affinities	58
PVDF-HFP	SiO_2	1 M $LiPF_6$–DMC/EC/EMC	—	3.45 mS cm^{-1}	Excellent interfacial compatibility and cyclic capacity retention	59
PEO	SiO_2	1 mole $LiPF_6$–DEC/EC	—	2 mS cm^{-1}	High performance Li-ionically conductor and consistent separator	60
PVDF	SiO_2–TiO_2	$LiPF_6$ or LiBOB	—	—	Increase in battery capacity	61
PEG	Al_2O_3	1 M $LiPF_6$–DMC/EC	—	0.93 mS cm^{-1}	Excellent cycling stability and good rate performance	62
PEO	—	LiTFSI and $PYR_{13}FSI$	—	2.43 mScm^{-1}	Electrochemical stability up to 4.5 V	63

developed a composite material by incorporating $Li_{10}GeP_2S_{12}$ (LGPS) in to a polyethylene oxide (PEO) matrix. This CPEs unveiled a highest ionic transport of 1.21×10^{-3} S cm^{-1} and showed enhanced electro-chemical durability of 0–5.7 V. In addition, they have also reported that the Li ion transport in this CPE was much faster at higher temperature (>50 °C), and slower at low temperatures (<50 °C).[65] The garnet type composite solid polymer electrolyte also shows good ionic conductivity and wide electrochemical window.[66]

When using the garnet type ceramic electrolyte, the electrode/electrolyte interface showed poor conductivity. It is due to their poor conductivity of the interface, the battery performance is often deteriorated. Hence, this garnet type generally increases the resistance at interfaces while the ionic conductivity is decreasing.[72] But the overall electrochemical performance is improved by the polymer/garnet type composite polymer electrolytes.[73] An example is the development of a PVDF/LLZTO composite hybrid polymer electrolyte, achieved

by introducing fast ionic conductive fillers into the polymer matrix. $Li_{6.75}$ $La_3Zr_{1.75}Ta_{0.25}O_{12}$ (LLZTO) into PVDF polymer matrix. The outcome was remarkable with an achieved ionic conductivity of 5×10^{-4} S cm^{-1}.[70,74] PEO/$LiClO_4$ ceramic composite polymer electrolyte was fabricated by incorporating the $Li_{0.33}La_{0.557}TiO_3$ nanowires in PEO matrix and the ionic conductivity was estimated to be 2.4×10^{-4} S cm^{-1} at 25 °C.[75] NASICON type ceramic polymer electrolytes[76,77] could be used in an ambient atmospheric condition as they are stable and possess the ionic conductivity over 10^{-3} S cm^{-1}. The PEO matrix incorporated with NASICON based ceramic $Li_{1.5}Al_{0.5}Ge_{1.5}(PO_4)_3$ exhibited the ionic mobility of 6.76×10^{-4} S cm^{-1}.[45]

Glasses, glass–ceramic and ceramics are the three different categories of sulfide type of ceramics. Thio-LISICON type electrolyte shows high ionic mobility and lower activation energy. Due to the higher ionic radius of the sulfides, it is showing enlarged ionic transport channels. Li_2S–P_2S_5, Li_2S-GeS_2, Li_2S–B_2S_3 and Li_2S–SiS_2 are the most commonly used sulfide glass electrolytes and they show ionic conductivity up to $\sim 10^{-4}$ S cm^{-1}.[64] Notably, it is reported that the heated Li_2S–P_2S_5 glass ceramics electrolyte displayed the ionic conductivity of 1.7×10^{-2} S cm^{-1}.[78] Similarly, the chlorine doped silicon-based sulfide composite polymer electrolyte ($Li_{9.54}Si_{1.74}P_{1.44}S_{11.7}Cl_{0.3}$) showed the highest ionic transport of 2.5×10^{-2} S cm^{-1}.[79] The network structure of many rapid ion conductors namely perovskite, metal-framework, crystals based and sulfide based nanoceramic are presented in Fig. 3f–i. Jin *et al.*, conducted reach on the compositional requirement of three key factors influencing ionic conductivity, ion transport pathways, ion mobility, and active ionic concentrations. Increasing the faction of LLZO ceramic in the LLZO–PEO composites, it decreased their ion mobilities and ion transport pathways transport from polymer to ceramic composites.[67] Li-ion transport behavior within the polymer nanoceramic composite (different percentages of LLZO on PEO/LITFSI) and their mechanism pathways also provided. Specifically, the study focused on a ^{6}Li NMR to determine the Li replacement behavior within the composite electrolytes. They observed that ^{6}Li enrichment in LiTFSI–PEO is found to be 23.3%, which indicating that Li ions traverse the PEO matrix to facilitate ion conductions as shown in Fig. 3a. Also, various fast ionically conductive ceramics are given in Table 2. Interestingly, Sun and colleagues used ALD to deposit a controlled, ultrathin LiNbOx (LNO) film on a NMC811 ($LiNi_{0.8}Co_{0.1}Mn_{0.1}O_2$) cathode and paired it with an LGPS electrolyte. This LNO interfacial layer stabilized the interface, demonstrated high bulk ionic conductivity (2.07×10^{-3} S cm^{-1}) and improved electrochemical performance (Fig. 4a–e). These enhancements show that the LNO film on NMC811 improves ionic conductivity and suppresses side reactions, leading to better electrochemical performance.[71] Similarly, Yao *et al.*, reported the doubled-layered solid composite electrolytes (DLSCE) for higher voltage solid Li metal battery.[68] The DLSCE was created by incorporating two different compositions into the electrolyte. The poly(vinylidene fluoride hexafluoropropylene) and 10 wt% of $Li_{1.3}A_{10.3}Ti_{1.7}(PO_4)_3$ (LATP) was used in cathode, whereas a Li friendly PEO–5 wt% LATP was prepared and contact with Li-metal and achieved 0.43 of high ionic transference number, redox window (4.82 V) and higher ionic transport (1.49×10^{-4} S cm^{-1}). The LSV and charge/discharge curve for obtained electrolyte are shown in Fig. 3b and c. During the electrochemical study there is no side reaction was observed by Yao and co-workers. Likewise, Bae *et al.*,

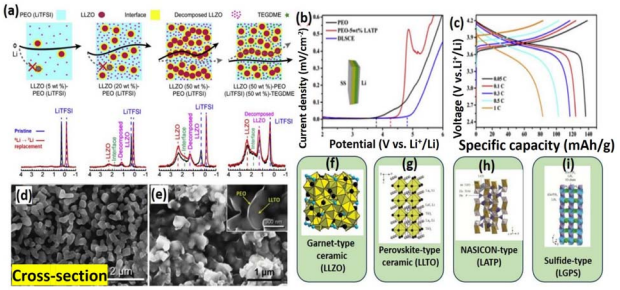

Fig. 3 (a) Schematic diagram of Li^+ conductive paths in a PEO–LiTFSI/LLZO CPE at different concentration of active fillers and their agreeing ^{6}Li NMR analysis.[67] Reproduced ref. 67 with permission from American Chemical Society, Copyright 2018, (b) LSVs data of double-layered CPE membranes compared with a single-layer of PEO–LiTFSI and LATP–PEO, (c) charge–discharge of an Li/DLSCE/NCM111 cell showing no side reaction in the cell.[68] Reproduced ref. 68 with permission from American Chemical Society, Copyright 2021, (d) LLTO framework (e) LLTO framework/PEO-LiTFSI CPE.[69] Reproduced ref. 69 with permission from Wiley-VCH Verlag GmbH & Co, Copyright 2018, (f) framework based garnet-type ceramic, (g) crystal based perovskite-type ceramic, (h) crystal based NASICON- type ceramic, and (i) Crystal based sulfide-type ceramic.[70] Reproduced ref. 70 with permission from Frontiers, Copyright 2019.

Table 2 Fast ionic conductive ceramics and polymer solid electrolytes

S. no.	Polymer electrolyte compositions	Ion conductivities (S cm^{-1})	Ref.
1	$Li_{0.33}La_{0.557}TiO_3$ (LLTO)–PEO–LiTFSI	2.4×10^{-4} (at RT)	80
2	20% $Li_{1.5}Al_{0.5}Ge_{1.5}(PO_4)_3$ (LAGP)–PEO–$LiFePO_4$	6.76×10^{-4} (60 °C)	81
3	$Li_{6.75}La_3Zr_{1.73}Ta_{0.23}O_{12}$–PVDF–$LiClO_4$	5×10^{-4} (25 °C)	82
4	$Li_{6.20}Ga_{0.30}La_{2.95}Rb_{0.05}Zr_2O_{12}$–PVDF–LiTFSI	1.62×10^{-3} (25 °C)	83
5	$Li_{0.33}La_{0.557}TiO_3$ (LLTO)–random nanowire–PAN–$LiClO_4$	2.4×10^{-4} (25 °C)	84
6	$Li_7La_3Zr_2O_{12}$ (LLZO)–PEO–$LiClO_4$	4.42×10^{-4} (55 °C)	85
7	$Li_{2.5}Al_{0.5}Ge_{1.5}(PO_4)_3$ (LAGP)–PEO–$LiClO_4$	2.6×10^{-4} (55 °C)	86
8	$Li_{6.7}La_3Zr_{1.7}Ta_{0.3}O_{12}$–PEO–LiTFSI	1.7×10^{-4} (30 °C)	87
9	7.5 wt% of $Li_7La_3Zr_2O_{12}$–PEO–LiTFSI	5.5×10^{-4} (30 °C)	88
10	$Li_{1.3}Al_{0.3}Ti_{1.7}(PO_4)_3$–PVDF–HFP–1 M $LiPF_6$–(EC/EMC/DMC)	3.943×10^{-3} (25 °C)	43

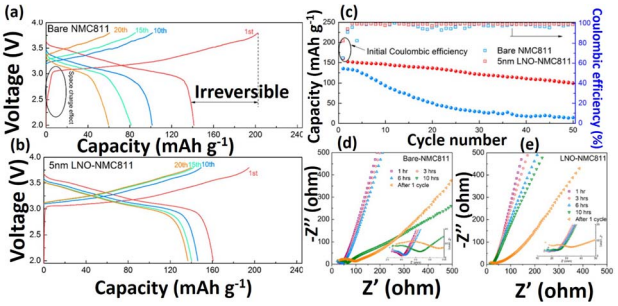

Fig. 4 Electrochemical studies of pristine and LNO coated NMC811 in SSLIBs (a and b) charge–discharge study, (c) cycling voltammetry performance study and (d and e) EIS studies of LIBs at a various inactive times and after the charge/discharge test studies.[71] Reproduced ref. 71 with permission from American Chemical Society, Copyright 2019.

finds on a high-performance composite polymer electrolyte based on hydrogel for SSLIBs.[69] The PEO matrix was fully covered the LLTO framework and their top view and cross-sectional view of composite electrolyte (percolated framework) was observed by SEM as shown in Fig. 3d and e. The outcome of this work was achieved their ionic conductivity (LLTO framework) up to 8.8×10^{-5} S cm^{-1}.

4. Exploring plasticizer based composite polymer electrolytes

Plasticizers play a vital role in composites polymer solid electrolytes by reducing the crystalline nature of the polymer matrix and increasing segmental mobility in terms of ion dissociation, enabling a high number of charge transporters for efficient ion transportation in the solid electrolyte. Typically, lower M_w polymers and non-volatile based organic solvents are used as plasticizers. Commonly used plasticizers, namely ethylene carbonate (EC), include propylene carbonate (PC), dimethyl carbonate (DMC), 1,2 dimethoxymethane (DME), ethyl methyl carbonate (EMC), dioctyl phthalate (DOP), dimethyl phthalate (DMP), dibutyl phthalate (BBP), dimethyl sulphoxide (DMSO), offer remarkable versatility and contribute to the impressive performance of plasticized composite polymer electrolytes.[89,90] In a different study, the polymer electrolytes system was prepared by incorporating a solid plasticizer known as succinonitrile (SCN) and a liquid plasticizer, tetraethylene glycol dimethyl ether (TEGDME). The role of plasticizers was found to be increased the ionic transport of the polymer network at a superionically conductive.[91] In another investigation, the combination of a considerable quantity of plasticizer in the polymer solid electrolyte was reported, where it enhanced the overall ionic transport of the composite polymer electrolyte. The incorporation of plasticizers to the polymer matrix was found to have transformative effect on composite polymer electrolyte. These plasticizers weaken the inter/intra molecular force within polymer chain, which dropping their active centers. Interestingly, the presence of lower molecular weight-based plasticizers, which decreases the glass transition temperatures. The reduction in temperature leads to decreased crystallinity within the polymer network. As the result, the electrolyte proves increased salt dissociation ability and enhanced overall charge carrier transportation.[92] Furthermore, the ionic transport of the polymer electrolyte is also found to be enhanced by incorporating a substantial amount of plasticizer. Notably, the plasticizer tends to transform the semi-crystalline phase of PVA host polymer to the amorphous phase. Accordingly, the literature reports show the PVA electrolytes containing $LiCLO_4$ and various plasticizers, two novel plasticizers, Triton (poly ethylene glycol *p-tert* octyl phenyl ether) and sulfolane (tetra methyl sulfone), were introduced.[93]

The sulfolane plasticizes based PVA–$LiClO_4$ matrix is found to be more effective than the Triton. Hence, the sulfolane plasticized solid polymer electrolytes show higher ionic conductivity than the Triton plasticized electrolytes. Another investigation reported that the PVA–chitosan blend matrix plasticized with 70 wt% of ethylene carbonates improve the ionic transport up to 10^{-3} S cm^{-1}. The charge carrier concentration values were found to be 6.57×10^{19} cm^{-3} and 2.20×10^{21} cm^{-3} for bare electrolyte and 70 wt% EC content respectively. Additionally, the mobility of EC plasticized electrolyte was found to be 4.54×10^{-6} cm^2 V^{-1} s^{-1}.[99] Ethylene carbonate-free electrolytes have also been used in batteries. It was also found that the crystalline phase and regular arrangement of morphologies were drastically changed into amorphous phase upon the addition of EC as a plasticizer. Various plasticized-composite based polymer electrolytes are shown in Table 3. Das *et al.*, also reported different charge carrier relaxation-based plasticizer PEO/PVDF-HFP electrolytes for solid batteries.[94] Interestingly, charge transporter reduction is highly non-exponential in plasticized based solid electrolytes during

Table 3 Various plasticized-composite based polymer electrolytes

S. no.	Electrolyte composition	Ionic conductivity	Ref.
1	PVA–PMMA–$LiBF_4$–ethylene carbonate	1.26×10^{-6} S cm^{-1}	96
2	PVA–PMMA–$LiClO_4$–dimethyl phthalate	6.0×10^{-4} S cm^{-1}	97
3	PVA–$LiClO_4$–dimethyl phthalate	1.49×10^{-3} S cm^{-1}	98
4	PVA–Chitosan–NH_4NO_3–ethylene carbonate	1.60×10^{-3} S cm^{-1}	99
5	$(PEO)_{40}$–$(LiCF_3SO_3)$ $(LiN[CF_3SO_2]_2)$–diethyl phthalate $(DEP)_5$	4.6×10^{-5} S cm^{-1}	100
6	PEO/PVDF–HFP–$LiClO_4$-50 wt% of ECs	1.40×10^{-6} S cm^{-1}	90 and 94
7	PEO/PVDF-HFP–$LiClO_4$-30 wt% of PCs	2.68×10^{-6} S cm^{-1}	94
8	PVDF-HFP + LiTf: EC (60 : 40)	$\sim 10^{-3}$ S cm^{-1}	101

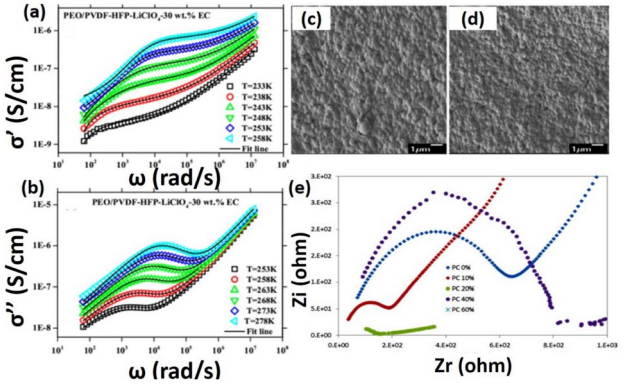

Fig. 5 (a) Real and (b) imaginary plots of conductivity at various temperatures for PEO/PVDF–HFP–$LiClO_4$-30 wt% ECs, FE-SEM images of (c) PEO/PVDF–HFP–$LiClO_4$-30 wt% PCs, (d) PEO/PVDF–HFP–$LiClO_4$-30 wt% DMCs polymer solid electrolytes.[94] Reproduced ref. 94 with permission from American Chemical Society, Copyright 2017, (e) impedance plot of PCL/$LiCF_3SO_3$ and PC plasticizer with different composition.[95] Reproduced ref. 95 with permission from Institute of Physics, Copyright 2020.

electrochemical analysis. The frequency requirements of the real (σ') and imaginary part (σ'') of conductivity (σ^*) for composites of PEO/PVDF–HFP–$LiClO_4$-30 wt% of EC based electrolyte at different temperatures are displayed in Fig. 5a and b. Fig. 4a reveals that at low frequency σ' declines quickly due to interfacial effect and polarization effects of electrode and it has high temperature σ', which corresponds to the DC conductivities. Particularly, σ'' shows a rapid increase with rise in frequency at high frequencies. As the frequency is reduced, σ'' also decreases at very low frequencies. FESEM images of the PEO/PVDF–HFP–$LiClO_4$ electrolytes and incorporation plasticizer were analyzed by FE-SEM and as shown in Fig. 5c and d.

From the analysis, they observed that the sponges-like uniform nanostructure with micropores/small spherulites in the electrolyte due to porous nanostructure of the PVDF–HFP. Interestingly, incorporation of EC plasticizer on the polymer matrix, reduces their crystalline phase and increases amorphous phase, which is suitable for excellent ion transport behavior. Similarly, Evi *et al.*, developed the polycaprolactone/$LiCF_3SO_3$ with added plasticizer for all solid-state batteries.[95] They have studied their electrical properties especially conductivity of the PCL based electrolytes with various concentration of PC plasticizer. Fig. 5e, shows a typical cole–cole plot containing title spiked at higher frequency, and depressed semicircle at lower frequency. Nurbol *et al.*,[102] reported that a (PAA/PEO)30 artificial protective texture was used as an interlayer between LATP and Li metal *via* a layer-by-layer polymer assembly technique. This interlayer exhibited excellent reversible electrochemical behaviour and stability up to 5 V, with nearly 100% coulombic efficiency. The link between PAA and PEO is based on intermolecular hydrogen bonding as shown in Fig. 6c. The negatively charged of PEI/PAA revealed that after 20 charge–discharge cycles, the LATP and polymer film maintained its uniformity (Fig. 6a). However, the ceramic grains developed large fractures (10–200 μm) due to chemical mechanical stress during cycling, which limited the operation of the ASSLB (see Fig. 6b).[102]

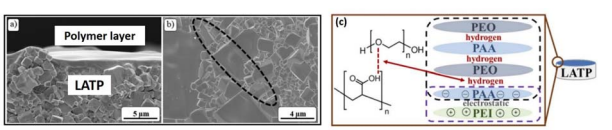

Fig. 6 After 20 cycles of SEM images of stripped ASSLB with a (PAA/PEO)30 films, (a) cross-section image of LATP and (PEO/PAA)30, (b) fractured film of LATP grains, and (c) film development mechanism between PEO, PAA, and PEI.[102] Reproduced ref. 102 with permission from Royal Society of Chemistry, Copyright 2022.

5. Nanoparticles or fillers-based composite polymer electrolytes

0D, 1D, and 2D nano-structured nanofillers[103,104] and surface improved nanofillers are also used in the synthesis of ferroelectric polymer composites. For instance, the ZrO_2, Al_2O_3, SiO_2, MgO are developed as 0D fillers with relatively low K value and used as insulating blocks to resist the dielectric breakdown and to decrease the leakage current. Carbon nanotubes are mostly used as a 1D filler and improve the dielectric constants as well. Boron nitride nanotubes and ceramic nanowires such as titanium dioxide (TiO_2) and $BaTiO_3$ (BT) are also incorporated into ferroelectric polymer matrix. Materials such as graphene oxide nanosheets (GO), molybdenum disulfide nanosheets (MoS_2), montmorillonite nanoplatelets are some of the examples for 2D fillers, which are successful used as electrolytes.[105] Ce-Wen *et al.*, fabricated the nanocomposite SiO_2 particles-incorporated composite polymer electrolyte, where the mesoporous SiO_2 was embedded with the ethylene carbonate/propylene carbonate as plasticizers and this developed EC/PC–SiO_2 nanocomposite was incorporated in the PEO–Li based PEO–Li/(EC/PC–SiO_2) electrolytes. These EC/PC–SiO_2 nanocomposite embedded EC/PC conducting nanochannels essentially provided the unique additional fast transport paths to achieve the enhanced conductivity.[106] The materials such as montmorillonite, clay and mica in the form of 2D mesoporous nanoplates are also used as fillers to achieve high performance CPEs. Interestingly, the ionic liquid functionalized mesoporous silica nanoplate showed an ionic transport of 1.8×10^{-5} S cm^{-1} at 20 °C,[107] where it was attributed to the continuous and extended pathway of the nanowires, which built the 3D network for the fast-ion transportation. Similarly, the nanowires of LLTO were combined in PAN–$LiClO_4$ composite polymer electrolyte, where it showed the ionic transport of 2.4×10^{-4} S cm^{-1}. Notably, this achieved range of ionic conductivity is three orders of higher magnitude as compared to that of the filler-free electrolytes.[108] In another study, it is demonstrated that an increase Lewis acid–base interaction area, which could be created when *in situ* hydrolysis, SiO_2 nanoparticles with precise size and higher monodispersity are established in the system. It is also observed that these mono-dispersed ultrafine SiO_2 spheres decreases the crystallinity of the PEO matrixes[109] and leads to the enhanced ionic transport up to 10^{-5} S cm^{-1}.[110]

6. Summary and future prospects

The main objective of the review is to highlight the transition from liquid electrolytes to solid electrolytes in lithium ion batteries. This is due to fact that these solid polymer electrolytes defend the batteries from internal short-circuiting and it also confirms the safety of the lithium ion batteries. The factors such as low flammability, good stability, thermal and high safety basically made the solid polymer electrolytes as the auspicious spare for the liquid-based electrolytes. The important attributes of these solid-electrolytes include that it should be mechanically and physically strong and it should be supportive for the continuous lithium ion movement without getting any structural damages or shrinkages. Further, it should also possess good electrochemical resistance as well. In this context, the CPEs such as polymer/fast-ion conductor-based CPEs, polymer/nano fillers or particle based composite electrolytes, polymer/inorganic ceramic based composite solid polymer electrolytes and plasticized composite polymer electrolytes were summarized. Even though significant works have been made on the progress of solid polymer-based electrolytes, it still needs some substantial efforts are required to overwhelmed the challenges in enhancing the electrochemical properties of the solid-polymer matrixes. The further research in this direction involves in enlightening the interfacial contacts in the SPEs, where the interfacial interaction and conductive mechanisms need to be clearly addressed to have better solid-state polymer electrolytes with enhanced properties.

Data availability

The data that support the findings of this study are available from the corresponding author upon reasonable request.

Author contributions

Writing original draft preparation, conceptualization and methodology: A. M.; formal analysis: R. R. and S. M.; funding, review and editing: S. J. P., S. S. H. and A. M. All authors have read and agreed to the published version of the manuscript.

Conflicts of interest

There are no conflicts to declare.

Acknowledgements

This research was supported by the National Research Foundation of Korea (NRF) (Grant No. 2020R1A6A1A03044512), Korea Institute of Planning and Evaluation for Technology in Food, Agriculture and Forestry (IPET) funded by Ministry of Agriculture, Food and Rural Affairs (MAFRA) (321027-5). The author (Dr A. Murali) also thankful to the Department of Science and Technology (DST), Govt. of India, grant no: DST/INSPIRE/04/2018/001762 for DST Inspire Faculty.

References

1 S. Mahmud, M. Rahman, M. Kamruzzaman, M. O. Ali, M. S. A. Emon, H. Khatun and M. R. Ali, *Results Eng.*, 2022, **15**, 100472, DOI: 10.1016/j.rineng.2022.100472.
2 F. Yu, S. Ge, B. Li, G. Sun, R. Mei and L. Zheng, *Curr. Inorg. Chem.*, 2012, **2**, 194–212.
3 A. Murali, M. Sakar, S. Priya, V. Vijayavarman, S. Pandey, R. Sai, Y. Katayama, M. Abdul Kader and K. Ramanujam, *Mater. Lett.*, 2022, **313**, 131764, DOI: 10.1016/j.matlet.2022.131764.
4 A. Murali, S. A. Vallal, M. Sakar, R. Ramesh, M. Devendiran and N. Suthanthira Vanitha, *Adv. Mater. Lett.*, 2021, **12**, 1–9.
5 H. Chen, M. Zheng, S. Qian, H. Y. Ling, Z. Wu, X. Liu, C. Yan and S. Zhang, *Carbon Energy*, 2021, **3**, 929–956, DOI: 10.1002/cey2.146.
6 M. S. Michael, M. M. E. Jacob, S. R. S. Prabaharan and S. Radhakrishna, *Solid State Ionics*, 1997, **98**, 167–174.
7 A. Chakrabarti, R. Filler and B. K. Mandal, *J. Solid State Electrochem.*, 2008, **12**, 269–272, DOI: 10.1007/s10008-007-0388-z.
8 K. Yongku, H. J. Kim, E. Kim, B. Oh and J. H. Cho, *J. Power Sources*, 2001, **92**, 255–259.
9 S. Ohta, T. Kobayashi and T. Asaoka, *J. Power Sources*, 2011, **196**, 3342–3345, DOI: 10.1016/j.jpowsour.2010.11.089.
10 S. Yu, R. D. Schmidt, R. Garcia-Mendez, E. Herbert, N. J. Dudney, J. B. Wolfenstine, J. Sakamoto and D. J. Siegel, *Chem. Mater.*, 2016, **28**, 197–206, DOI: 10.1021/acs.chemmater.5b03854.
11 J. H. Cha, P. N. Didwal, J. M. Kim, D. R. Chang and C. J. Park, *J. Membr. Sci.*, 2020, **595**, 117538, DOI: 10.1016/j.memsci.2019.117538.
12 Y. Zhang, R. Chen, S. Wang, T. Liu, B. Xu, X. Zhang, X. Wang, Y. Shen, Y. H. Lin, M. Li, L. Z. Fan, L. Li and C. W. Nan, *Energy Storage Mater.*, 2020, **25**, 145–153, DOI: 10.1016/j.ensm.2019.10.020.
13 A. K. Kenessova, G. A. Seilkhanova, T. S. Kurmanbayeva, E. Z. Ussipbekova and A. P. Kurbatov, *Mater. Today: Proc.*, 2020, **31**, 588–591, DOI: 10.1016/j.matpr.2020.07.106.
14 J. R. Kim, S. W. Choi, S. M. Jo, W. S. Lee and B. C. Kim, *Electrochim. Acta*, 2004, **50**, 69–75, DOI: 10.1016/j.electacta.2004.07.014.
15 X. Zhu, X. Jiang, X. Ai, H. Yang and Y. Cao, *J. Membr. Sci.*, 2016, **504**, 97–103, DOI: 10.1016/j.memsci.2015.12.059.
16 S. Suriyakumar, M. Raja, N. Angulakshmi, K. S. Nahm and A. M. Stephan, *RSC Adv.*, 2016, **6**, 92020–92027, DOI: 10.1039/c6ra19168a.
17 Z. Wang, Y. Xie, C. Xu, S. Shi, L. Wang, G. Zhang, X. Wang, L. Zhu and D. Xu, *J. Solid State Electrochem.*, 2019, **23**, 269–276, DOI: 10.1007/s10008-018-4132-7.
18 S. Wu, J. Ning, F. Jiang, J. Shi and F. Huang, *ACS Omega*, 2019, **4**, 16309–16317, DOI: 10.1021/acsomega.9b01541.
19 N. D. A. Aziz, N. Kamarulzaman, R. H. Y. Subban, A. S. Hamzah, A. Z. Ahmed, Z. Osman, R. Rusdi, N. Kamarudin, N. Mohalid, A. Z. Romli and Z. Shaameri,

AIP Conf. Proc., 2017, **1877**, 060007, DOI: 10.1063/1.4999886.
20 A. Emre, M. H. Uğur and N. Kayaman-Apohan, *Polym. Adv. Technol.*, 2017, **28**, 1951–1960, DOI: 10.1002/pat.4086.
21 W. Jiayu, J. Xie, X. Kong, Z. Liu, K. Liu, F. Shi, A. Pei, H. Chen, W. Chen, J. Chen, X. Zhang, L. Zong, J. Wang, L. Q. Chen, J. Qin and Y. Cui, *Nat. Nanotechnol.*, 2019, **14**, 705–711, DOI: 10.1038/s41565-019-0465-3.
22 L. Wang, F. Liu, W. Shao, S. Cui, Y. Zhao, Y. Zhou and J. He, *Compos. Commun.*, 2019, **16**, 150–157, DOI: 10.1016/j.coco.2019.09.004.
23 Z. Li, W. Wang, Y. Han, L. Zhang, S. Li, B. Tang, S. Xu and Z. Xu, *J. Power Sources*, 2018, **378**, 176–183, DOI: 10.1016/j.jpowsour.2017.12.018.
24 L. Long, S. Wang, M. Xiao and Y. Meng, *J. Mater. Chem. A*, 2016, **4**, 10038–10039, DOI: 10.1039/c6ta02621d.
25 J. W. Fergus, *J. Power Sources*, 2010, **195**, 4554–4569, DOI: 10.1016/j.jpowsour.2010.01.076.
26 G. Lu, J. Li, J. Ju, L. Wang, J. Yan, B. Cheng, W. Kang, N. Deng and Y. Li, *J. Chem. Eng.*, 2020, **389**, 124478, DOI: 10.1016/j.cej.2020.124478.
27 Z. Yang, J. Fan, W. Xu, Z. Yang, J. Zeng and X. Cao, *Ind. Eng. Chem. Res.*, 2022, **61**, 4850–4859, DOI: 10.1021/acs.iecr.2c00450.
28 J. R. Nair, L. Porcarelli, F. Bella and C. Gerbaldi, *ACS Appl. Mater. Interfaces*, 2015, **7**, 12961–12971, DOI: 10.1021/acsami.5b02729.
29 B. Azhar, Q. T. Pham, Y. S. Wu, C. C. Yang, H. T. Wu, S. H. Huang and C. S. Chern, *Electrochim. Acta*, 2024, **480**, 143920, DOI: 10.1016/j.electacta.2024.143920.
30 B. Azhar, Q. T. Pham, M. Afiandika and C. S. Chern, *ACS Appl. Energy Mater.*, 2023, **6**, 3525–3537, DOI: 10.1021/acsaem.3c00154.
31 Q. T Pham, B. Azhar and C. S. Chern, *ECS Meeting Abstracts*, 2022, vol. 2, pp. 160, DOI: 10.1149/MA2022-012160mtgabs.
32 Q. Hu, S. Osswald, R. Daniel, Y. Zhu, S. Wesel, L. Ortiz and D. R. Sadoway, *J. Power Sources*, 2011, **196**, 5604–5610, DOI: 10.1016/j.jpowsour.2011.03.001.
33 P. E. Trapa, Y. Y. Won, S. C. Mui, E. A. Olivetti, B. Huang and D. R. Sadoway, *J. Electrochem. Soc.*, 2014, **152**(1), A1, DOI: 10.1149/1.1824032.
34 K. Khan, M. B. Hanif, H. Xin, A. Hussain, H. G. Ali, B. Fu, *et al.*, *Small*, 2024, **20**, 2305772, DOI: 10.1002/smll.202305772.
35 Z. Wang, Y. Hou, S. Li, Z. Xu, X. Zhu, B. Guo, K. Wang, *et al.*, *Small Struct.*, 2024, 2400050, DOI: 10.1002/sstr.202400050.
36 K. Daems, P. Yadav, K. B. Dermenci, J. Van Mierlo and M. Berecibar, *Renewable Sustainable Energy Rev.*, 2024, **191**, 114136, DOI: 10.1016/j.rser.2023.114136.
37 E. Samuilova, A. Ponomareva, V. Sitnikova, A. Zhilenkov, O. Kichigina and M. Uspenskaya, *Polymers*, 2024, **16**, 1551, DOI: 10.3390/polym16111551.
38 D. Zhou, D. Shanmukaraj, A. Tkacheva, M. Armand and G. Wang, *Chem*, 2019, **5**, 2326–2352, DOI: 10.1016/j.chempr.2019.05.009.
39 M. Sasikumar, M. Raja, R. H. Krishna, A. Jagadeesan, P. Sivakumar and S. Rajendran, *J. Phys. Chem. C*, 2018, **122**, 25741–25752, DOI: 10.1021/acs.jpcc.8b03952.
40 J. Zhang, X. Huang, H. Wei, J. Fu, Y. Huang and X. Tang, *J. Solid State Electrochem.*, 2012, **16**, 101–107, DOI: 10.1007/s10008-010-1278-3.
41 E. M. Masoud, A. A. El-Bellihi, W. A. Bayoumy and M. A. Mousa, *J. Alloys Compd.*, 2013, **575**, 223–228, DOI: 10.1016/j.jallcom.2013.04.054.
42 G. Wang, X. Zhu, A. Rashid, Z. Hu, P. Sun, Q. Zhang and L. Zhang, *J. Mater. Chem. A*, 2020, **8**, 13351–13363, DOI: 10.1039/d0ta00335b.
43 Y. Wang, S. Wang, J. Fang, L. X. Ding and H. Wang, *J. Membr. Sci.*, 2017, **537**, 248–254, DOI: 10.1016/j.memsci.2017.05.023.
44 J. Shayapat, O. H. Chung and J. S. Park, *Electrochim. Acta*, 2015, **170**, 110–121, DOI: 10.1016/j.electacta.2015.04.142.
45 Q. Wang, W. L. Song, L. Wang, Y. Song, Q. Shi and L. Z. Fan, *Electrochim. Acta*, 2014, **132**, 538–544, DOI: 10.1016/j.electacta.2014.04.053.
46 S. Yang, W. Ma, A. Wang, J. Gu and Y. Yin, *RSC Adv.*, 2018, **8**, 23390–23396, DOI: 10.1039/C8RA02035C.
47 G. Zainab, X. Wang, J. Yu, Y. Zhai, A. Ahmed Babar, K. Xiao and B. Ding, *Mater. Chem. Phys.*, 2016, **182**, 308–314, DOI: 10.1016/j.matchemphys.2016.07.037.
48 Z. Liu, W. Jiang, Q. Kong, C. Zhang, P. Han, X. Wang, J. Yao and G. Cui, *Macromol. Mater. Eng.*, 2013, **298**, 806–813, DOI: 10.1002/mame.201200158.
49 S. Park, C. W. Son, S. Lee, D. Y. Kim, C. Park, K. S. Eom, T. F. Fuller, H. I. Joh and S. M. Jo, *Sci. Rep.*, 2016, **6**, 36977, DOI: 10.1038/srep36977.
50 Y. Li, X. Wang, J. Liang, K. Wu, L. Xu and J. Wang, *Polymers*, 2020, **12**, 12040764, DOI: 10.3390/POLYM12040764.
51 O. Padmaraj, B. N. Rao, M. Venkateswarlu and N. Satyanarayana, *J. Phys. Chem. B*, 2015, **119**, 5299–5308, DOI: 10.1021/jp5115477.
52 Q. Fu, G. Lin, X. Chen, Z. Yu, R. Yang, M. Li, X. Zeng and J. Chen, *Energy Technol.*, 2018, **6**, 144–152, DOI: 10.1002/ente.201700347.
53 M. Yanilmaz, Y. Lu, J. Zhu and X. Zhang, *J. Power Sources*, 2016, **313**, 205–212, DOI: 10.1016/j.jpowsour.2016.02.089.
54 M. Yanilmaz, Y. Lu, M. Dirican, K. Fu and X. Zhang, *J. Membr. Sci.*, 2014, **456**, 57–65, DOI: 10.1016/j.memsci.2014.01.022.
55 C. Fang, S. Yang, X. Zhao, P. Du and J. Xiong, *Mater. Res. Bull.*, 2016, **79**, 1–7, DOI: 10.1016/j.materresbull.2016.02.015.
56 M. Yanilmaz, M. Dirican and X. Zhang, *Electrochim. Acta*, 2014, **133**, 501–508, DOI: 10.1016/j.electacta.2014.04.109.
57 M. Yanilmaz, J. Zhu, Y. Lu, Y. Ge and X. Zhang, *J. Mater. Sci.*, 2017, **52**(1), 5232–5241, DOI: 10.1007/s10853-017-0764-8.
58 J. Zhang, Y. Xiang, M. I. Jamil, J. Lu, Q. Zhang, X. Zhan and F. Chen, *J. Membr. Sci.*, 2018, **564**, 753–761, DOI: 10.1016/j.memsci.2018.07.056.
59 S. Zhang, J. Cao, Y. Shang, L. Wang, X. He, J. Li, P. Zhao and Y. Wang, *J. Mater. Chem. A*, 2015, **3**, 17697–17703, DOI: 10.1039/c5ta02781k.

60 C. H. Tsao, Y. H. Hsiao, C. H. Hsu and P. L. Kuo, *ACS Appl. Mater. Interfaces*, 2016, **8**, 15216–15224, DOI: **10.1021/acsami.6b02345**.
61 Q. Sabrina, N. Majid and B. Prihandoko, *J. Phys.: Conf. Ser.*, 2016, **776**, 012062, DOI: **10.1088/1742-6596/776/1/012062**.
62 Y. Zhang, Z. Wang, H. Xiang, P. Shi and H. Wang, *J. Membr. Sci.*, 2016, **509**, 19–26, DOI: **10.1016/j.memsci.2016.02.047**.
63 E. Simonetti, M. Carewska, M. Di Carli, M. Moreno, M. De Francesco and G. B. Appetecchi, *Electrochim. Acta*, 2017, **235**, 323–331, DOI: **10.1016/j.electacta.2017.03.080**.
64 S. Xia, X. Wu, Z. Zhang, Y. Cui and W. Liu, *Chem*, 2019, **5**, 753–785, DOI: **10.1016/j.chempr.2018.11.013**.
65 Z. Li, W. X. Sha and X. Guo, *ACS Appl. Mater. Interfaces*, 2019, **11**, 26920–26927, DOI: **10.1021/acsami.9b07830**.
66 J. F. Wu, W. K. Pang, V. K. Peterson, L. Wei and X. Guo, *ACS Appl. Mater. Interfaces*, 2017, **9**, 12461–12468, DOI: **10.1021/acsami.7b00614**.
67 Z. Jin and Y. Y. Hu, *ACS Appl. Mater. Interfaces*, 2018, **10**, 4113–4120, DOI: **10.1021/acsami.7b17301**.
68 Z. Yao, K. Zhu, X. Li, J. Zhang, J. Li, J. Wang, K. Yan and J. Liu, *ACS Appl. Mater. Interfaces*, 2021, **13**, 11958–11967, DOI: **10.1021/acsami.0c22532**.
69 J. Bae, Y. Li, J. Zhang, X. Zhou, F. Zhao, Y. Shi, J. B. Goodenough and G. Yu, *Angew. Chem.*, 2018, **57**, 2096–2100, DOI: **10.1002/ange.201710841**.
70 P. Yao, H. Yu, Z. Ding, Y. Liu, J. Lu, M. Lavorgna, J. Wu and X. Liu, *Front. Chem.*, 2019, **7**, 522, DOI: **10.3389/fchem.2019.00522**.
71 X. Li, Z. Ren, M. Norouzi Banis, S. Deng, Y. Zhao and X. Sun, *ACS Energy Lett.*, 2019, **4**, 2480–2488, DOI: **10.1021/acsenergylett.9b01676**.
72 A. De Bruyne, K. Cérdan, G. O'Rourke, W. Stuyck, J. Leinders, M. Denayer, *et al.*, *ACS Appl. Polym. Mater.*, 2024, **6**, 6831–6842, DOI: **10.1021/acsapm.4c00809**.
73 L. Chen, Y. Li, S. P. Li, L. Z. Fan, C. W. Nan and J. B. Goodenough, *Nano Energy*, 2018, **46**, 176–184, DOI: **10.1016/j.nanoen.2017.12.037**.
74 X. Zhang, T. Liu, S. Zhang, X. Huang, B. Xu, Y. Lin, B. Xu, L. Li, C. W. Nan and Y. Shen, *J. Am. Chem. Soc.*, 2017, **139**, 13779–13785, DOI: **10.1021/jacs.7b06364**.
75 P. Zhu, C. Yan, M. Dirican, J. Zhu, J. Zang, R. K. Selvan, C. C. Chung, H. Jia, Y. Li, Y. Kiyak, N. Wu and X. Zhang, *J. Mater. Chem. A*, 2018, **6**, 4279–4285, DOI: **10.1039/c7ta10517g**.
76 L. Chayal, S. El Arni, M. Saadi, A. Assani, L. Bih, J. Ma and M. Hadouchi, *RSC Adv.*, 2024, **14**, 22159–22168, DOI: **10.1039/D4RA03529A**.
77 L. Han, C. T. Hsieh, B. C. Mallick, J. Li and Y. A. Gandomi, *Nanoscale Adv.*, 2021, **3**, 2728–2740, DOI: **10.1039/D0NA01072C**.
78 Y. Seino, T. Ota, K. Takada, A. Hayashi and M. Tatsumisago, *Energy Environ. Sci.*, 2014, **7**, 627–631, DOI: **10.1039/c3ee41655k**.
79 Y. Kato, S. Hori, T. Saito, K. Suzuki, M. Hirayama, A. Mitsui, M. Yonemura, H. Iba and R. Kanno, *Nat. Energy*, 2016, **1**, 30, DOI: **10.1038/nenergy.2016.30**.
80 P. Zhu, C. Yan, M. Dirican, J. Zhu, J. Zang, R. K. Selvan, C. C. Chung, H. Jia, Y. Li, Y. Kiyak, N. Wu and X. Zhang, *J. Mater. Chem. A*, 2018, **6**, 4279–4285, DOI: **10.1039/c7ta10517g**.
81 Y. Zhao, Z. Huang, S. Chen, B. Chen, J. Yang, Q. Zhang, F. Ding, Y. Chen and X. Xu, *Solid State Ionics*, 2016, **295**, 65–71, DOI: **10.1016/j.ssi.2016.07.013**.
82 L. J. A. Siqueira and M. C. C. Ribeiro, *J. Chem. Phys.*, 2006, **125**, 214903, DOI: **10.1063/1.2400221**.
83 B. Scrosati and J. Garche, *J. Power Sources*, 2010, **195**, 2419–2430, DOI: **10.1016/j.jpowsour.2009.11.048**.
84 S. Subianto, M. K. Mistry, N. R. Choudhury, N. K. Dutta and R. Knott, *ACS Appl. Mater. Interfaces*, 2009, **1**, 1173–1182, DOI: **10.1021/am900020w**.
85 Q. X. Shi, Q. Xia, X. Xiang, Y. S. Ye, H. Y. Peng, Z. G. Xue, X. L. Xie and Y. W. Mai, *Chem.–Eur. J.*, 2017, **23**, 11881–11890, DOI: **10.1002/chem.201702079**.
86 M. D. Tikekar, S. Choudhury, Z. Tu and L. A. Archer, *Nat. Energy*, 2016, **1**, 114, DOI: **10.1038/nenergy.2016.114**.
87 Z. Zhang, Y. Huang, H. Gao, J. Huang, C. Li and P. Liu, *Ceram. Int.*, 2020, **46**, 11397–11405, DOI: **10.1016/j.ceramint.2020.01.170**.
88 F. Chen, D. Yang, W. Zha, B. Zhu, Y. Zhang, J. Li, Y. Gu, Q. Shen, L. Zhang and D. R. Sadoway, *Electrochim. Acta*, 2017, **258**, 1106–1114, DOI: **10.1016/j.electacta.2017.11.164**.
89 W. Xu and C. A. Angell, *Electrochim. Acta*, 2003, 2029–2035, DOI: **10.1016/S0013-4686(03)00182-8**.
90 M. S. Michael, M. M. E. Jacob, S. R. S. Prabaharan and S. Radhakrishna, *Solid State Ionics*, 1997, **98**, 167–174.
91 H. Ruixuan, Studies on Ionic Conductivity and Electrochemical Stability of Plasticized Photopolymerized Polymer Electrolyte Membranes for Solid State Lithium Ion Batteries, PhD thesis, University of Akron, 2016.
92 S. B. Aziz, T. J. Woo, M. F. Z. Kadir and H. M. Ahmed, *J. Sci.: Adv. Mater. Devices*, 2018, **3**, 1–17, DOI: **10.1016/j.jsamd.2018.01.002**.
93 G. Hirankumar and N. Mehta, *Heliyon*, 2018, **4**, 992, DOI: **10.1016/j.heliyon.2018**.
94 S. Das and A. Ghosh, *J. Phys. Chem. B*, 2017, **121**, 5422–5432, DOI: **10.1021/acs.jpcb.7b02277**.
95 Y. Evi, Sudaryanto, Deswita and Wahyudianingsih, *IOP Conf. Ser.: Mater. Sci. Eng.*, 2020, **924**, 012034, DOI: **10.1088/1757-899X/924/1/012034**.
96 S. Rajendran, M. Sivakumar and R. Subadevi, *Mater. Lett.*, 2004, **58**, 641–649, DOI: **10.1016/S0167-577X(03)00585-8**.
97 S. Rajendran, M. Sivakumar and R. Subadevi, *Solid State Ionics*, 2004, **167**, 335–339, DOI: **10.1016/j.ssi.2004.01.020**.
98 K. H. Teoh, C. S. Lim and S. Ramesh, *Measurement*, 2014, **48**, 87–95, DOI: **10.1016/j.measurement.2013.10.040**.
99 M. F. Z. Kadir, S. R. Majid and A. K. Arof, *Electrochim. Acta*, 2010, **55**, 1475–1482, DOI: **10.1016/j.electacta.2009.05.011**.
100 C. W. Walker Jr and M. Salomon, *J. Electrochem. Soc.*, 1993, **140**, 3409, DOI: **10.1149/1.2221103**.
101 S. Ramesh and O. P. Ling, *Polym. Chem.*, 2010, **1**, 702–707, DOI: **10.1039/b9py00244h**.

102 T. Nurbol, M. Sarsembina, A. Nurpeissova, K. Kanamura, Z. Bakenov and A. Mentbayeva, *Nanoscale Adv.*, 2022, **4**, 4606, DOI: **10.1039/D2NA00521B**.

103 A. Murali, R. S. Babu, M. Sakar, S. Priya, R. Vinodh, K. P. Bhuvana, *et al.*, Bioinspired Nanomaterials for Supercapacitor Applications, *Bioinspired Nanomaterials for Energy and Environmental Applications*, 2022, vol. 121, pp. 141–174, DOI: **10.21741/9781644901836-5**.

104 A. Murali, S. Srinivasan, B. Appukutti Achuthan, M. Sakar, S. Chandrasekaran, N. Suthanthira Vanitha, R. Joseph Bensingh, M. Abdul Kader and S. N. Jaisankar, *Polymers*, 2020, **874**, 12, DOI: **10.3390/polym12040874**.

105 H. Li, F. Liu, B. Fan, D. Ai, Z. Peng and Q. Wang, *Small Methods*, 2018, **2**, 1700399, DOI: **10.1002/smtd.201700399**.

106 N. Ce-wen, L. Fan, Y. Lin and Q. Cai, *Phys. Rev. Lett.*, 2003, **91**, 266104, DOI: **10.1103/PhysRevLett.91.266104**.

107 S. Wang, Q. X. Shi, Y. S. Ye, Y. Wang, H. Y. Peng, Z. G. Xue, X. L. Xie and Y. W. Mai, *Electrochim. Acta*, 2017, **245**, 1010–1022, DOI: **10.1016/j.electacta.2017.05.125**.

108 W. Liu, N. Liu, J. Sun, P. C. Hsu, Y. Li, H. W. Lee and Y. Cui, *Nano Lett.*, 2015, **15**, 2740–2745, DOI: **10.1021/acs.nanolett.5b00600**.

109 J. Shen, S. Liu, D. Bian, Z. Chen, H. Pan, C. Yang, *et al.*, *Electrochim. Acta*, 2023, **456**, 142482, DOI: **10.1016/j.electacta.2023.142482**.

110 D. Lin, W. Liu, Y. Liu, H. R. Lee, P. C. Hsu, K. Liu and Y. Cui, *Nano Lett.*, 2016, **16**, 459–465, DOI: **10.1021/acs.nanolett.5b04117**.